Ore Geology Reviews 104 (2019) 620–627

Contents lists available at ScienceDirect

Ore Geology Reviews

journal homepage: www.elsevier.com/locate/oregeorev

Short communication

Pyrite Re-Os geochronology of the Sareke sediment-hosted Cu deposit, Xinjiang, NW China

Lu-Tong Zhao[a,*], Jing-Bin Wang[a], Yu-Wang Wang[a], Xin-You Zhu[a], Chao Li[b]

[a] Beijing Institute of Geology for Mineral Resources, Beijing 100012, China
[b] National Research Center of Geoanalysis, Chinese Academy of Geological Sciences, Beijing 100037, China

ARTICLE INFO

Keywords:
Pyrite Re-Os
Sediment-hosted stratabound copper deposit
Sareke
Western Tarim

ABSTRACT

The Sareke Cu deposit in the western Tarim region (Xinjiang, NW China) is hosted in continental sedimentary rocks of the Upper Jurassic Kuzigongsu Formation and Lower Cretaceous Kezilesu Group. Stratabound orebodies occur mainly in conglomerate and minor in siltstone. Both stratabound (major) and vein type (minor) ores are composed of chalcocite, chalcopyrite, bornite and pyrite with minor sphalerite and galena, which show a zonation pattern of chalcocite → chalcopyrite → sphalerite + galena → pyrite from north to south of Sareke. Carbonation is the most important hydrothermal alteration at Sareke and dolomite together with calcite are the dominant gangue minerals.

Six pyrite samples which coexist closely with copper sulfides are Re-Os dated and yielded a Re-Os isochron age of 115.8 ± 4.7 Ma and a weighted mean age of 114.3 ± 1.8 Ma, which constrain the Sareke Cu mineralization to the late Early Cretaceous. This age is synchronous with the tectonic inversion event and the basaltic magma activities of the Tuyon basin, which could been sources of dynamics and thermodynamics during the ore-forming process. This is the first unambiguous evidence for an appreciable copper concentration of Mesozoic age, and based on this evidence, additional Mesozoic sediment-hosted stratabound copper mineralization event may have occurred elsewhere within basins along the Talas-Fergana fault.

1. Introduction

Sediment-hosted stratabound copper (SSC) deposits are important sources of Cu, Co and Ag, and are commonly considered to form during the entire evolutionary history of a rift basin (Hitzman et al., 2005, 2010), whereas the timing of mineralization relative to sedimentation of the host sequence remains elusive for most deposits. Previous Re-Os geochronology attempts were focused mainly on the ancient (~1700 to 450 Ma) marine SSC deposits, and suggested that mineralization may postdate ore-hosting strata by up to hundreds of millions of years (Selley et al., 2005; Hitzman et al., 2005, 2010, 2012; Sillitoe, 2012; Huang et al., 2013; Zhao et al., 2013; Muchez et al., 2015; Perelló et al., 2015; Sillitoe et al., 2010, 2015).

This contribution reports a younger, unequivocal pyrite Re-Os mineralization age for a continental SSC deposit at Sareke, sourthern Xinjiang. The paper briefly describes the stratigraphic setting of Sareke and the Cu mineralization characteristics. In addition, we correlate the mineralization with regional geotectonic events during the evolution of the Tuyon basin, and speculate on possible correlations with the Early Cretaceous regional magmatic activities.

The sediment-hosted stratabound Sareke Cu deposit (15 km northwest of Wuqia County) is located in the western Tarim area (Fig. 1A). The ore-bearing Sarekebayi basin is a sub-basin of the Tuyon pull-apart basin (Fig. 1B). At present, the deposit contains an ore reserve of 79.54 Mt at 0.77% Cu and a small amount of Ag, Pb and Zn (Liu et al., 2016).

2. Regional geological setting

The western Tarim is located between the Southern Tianshan and Western Kunlun orogens (Fig. 1A), and can be subdivided into the Tuyon basin, the Sulutielke uplift and the Kashi depression (only northwestern part), with each terrane consisting of different stratigraphic combinations (Fig. 1B). The Sulutielke uplift is dominated by Mesoproterozoic gneiss, which constitutes also the basement of the Tuyon basin and the Kashi depression. The Jurassic alluvial/lacustrine coal-bearing successions were mainly developed within the Tuyon basin, among of the Upper Jurassic Formation hosts the Sarek Cu deposit. The Lower Cretaceous sandstone, conglomerate and mudstone that deposited in alluvial and braided river environments are widespread around the margin of Kashi depression and Tuyon basin, and

* Corresponding author.
E-mail address: zhaolutong0123@163.com (L.-T. Zhao).

https://doi.org/10.1016/j.oregeorev.2018.11.029
Received 14 May 2018; Received in revised form 23 November 2018; Accepted 30 November 2018
Available online 01 December 2018
0169-1368/

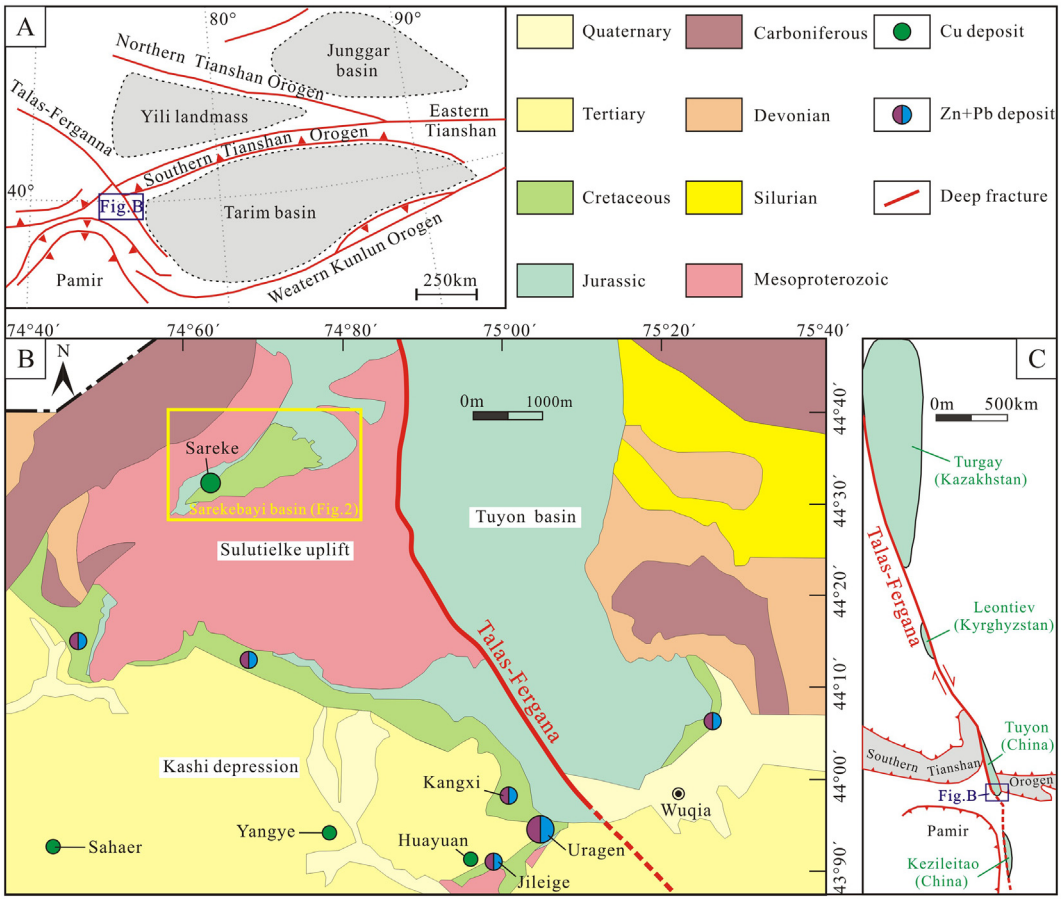

Fig. 1. (A) Geotectonic locations of Tarim basin, Southern Tianshan and Western Kunlun orogens (modified after Xue et al., 2014); (B) Regional geologic map of the western Tarim (modified after Fang et al., 2016); (C) The locations of Jurassic basins along the Talas-Fergana fault (modified after Li and Wang, 2008).

hosted a number of sandstone-hosted Zn-Pb deposits, including Uragen (super-large, 10Mt; Xue et al., 2014), Kangxi, and Jileige. From Late Cretaceous to Paleogene, the Kashi depression was subjected to a widespread marine transgression, forming a succession of transitional-marine and marine clastic rocks, carbonates and evaporates. Meanwhile, lacking of sedimentation but a large amount of basaltic magma activities is the most characteristic feature of the Tuyon basin (Bazhenov and Mikolaichuk, 2000; Sobel and Arnaud, 2000; Gilder et al., 2003; Xu et al., 2003; Liang et al., 2007). In the Neogene, the Kashi depression accumulated thick layers of lacustrine and fluvial red beds, which host the SSC deposits such as Huayuan and Yangye.

Major regional structures include a series of ENE–/SE–trending faults, with the most important one being the Talas-Fergana dextral strike-slip fault. The Talas-Fergana fault is one of the most important faults in Central Asia, and may have reactivated from the end Triassic and to the Early Cretaceous, opening a series of Jurassic basins (e.g., Turgay, Kazakhstan; Leontiev, Kyrghyzstan; Tuyon and Kezileitao, China) along the fault (Fig. 1C, Koserav et al., 1993; Allen et al., 2001; Luo et al., 2004, 2005).

3. Ore deposit geology

3.1. Stratigraphy, structure and intrusions

The stratigraphic system of the Sarekebayi basin is composed of two parts: the Mesoproterozoic Akesu Group basement and the overlying Mesozoic units (Fig. 2). The Mesoproterozoic Akesu Group is divided into six sub-groups, but only the upper three (the fourth to sixth) were found in Sarekbayi basin. The Mesozoic units include, from bottom to top, the Lower Jurassic Shalitashi and Kangsu Formations, Middle Jurassic Yangye and Taerduo Formations, Upper Jurassic Kuzigongsu Formation, and the Lower Cretaceous Kezilesu Group.

The Kezilesu Group is divided into five members, but only the lower three (the first to third) were found in the Sarekbayi basin. Their lithologies, from lower to upper, are described as follows. The basal member mainly consists of mudstone with intercalated sandstone and conglomerate, the middle member is consisted mainly of pebbly sandstone and siltstones, whereas the upper member is dominated by the conglomerate, celadon pebbly sandstone and quartzarenite with thin silty mudstone interbed. The Upper Jurassic Kuzigongsu Formation involves two members, of which the basal member is characterized by the presence of conglomerate, siltstone interbedded with pelitic siltstone, and a 2 m thick red-purple silty mudstone on its top stably. The upper member is consisted mainly of the conglomerate locally interbedded with sandstone lenses. Lithologies of the stratigraphic units are illustrated in Fig. 3.

The Sarekbayi basin is a NE–trending, generally west plunging syncline (Fig. 2). The northern limb dips to SE at a dip angle of 45°–65°, whereas the southern limb dips to the NW with dip angles of 15°–25°. The north and south boundary fault (F_1 and F_2; Fig. 2) are the most important faults in Sarekbayi basin, which thrusted the Mesoproterozoic Akesu Group over the Mesozoic units and caused the lack of sedimentary rocks in the southern limb. Faults of F_3 to F_7 occurred as boundary fault of sub-groups of Mesoproterozoic units and were mainly NE-trending. A few NE- and NEE-trending faults (F_8 to F_{21}; Fig. 2) were also developed north of the hinge of the syncline and crosscut the Mesozoic units and orebodies, indicating they were post-mineralization.

About 20 diabase dikes were documented at the southern part of the Sarekbayi basin (Fig. 2). These diabase dikes intruded the basal and

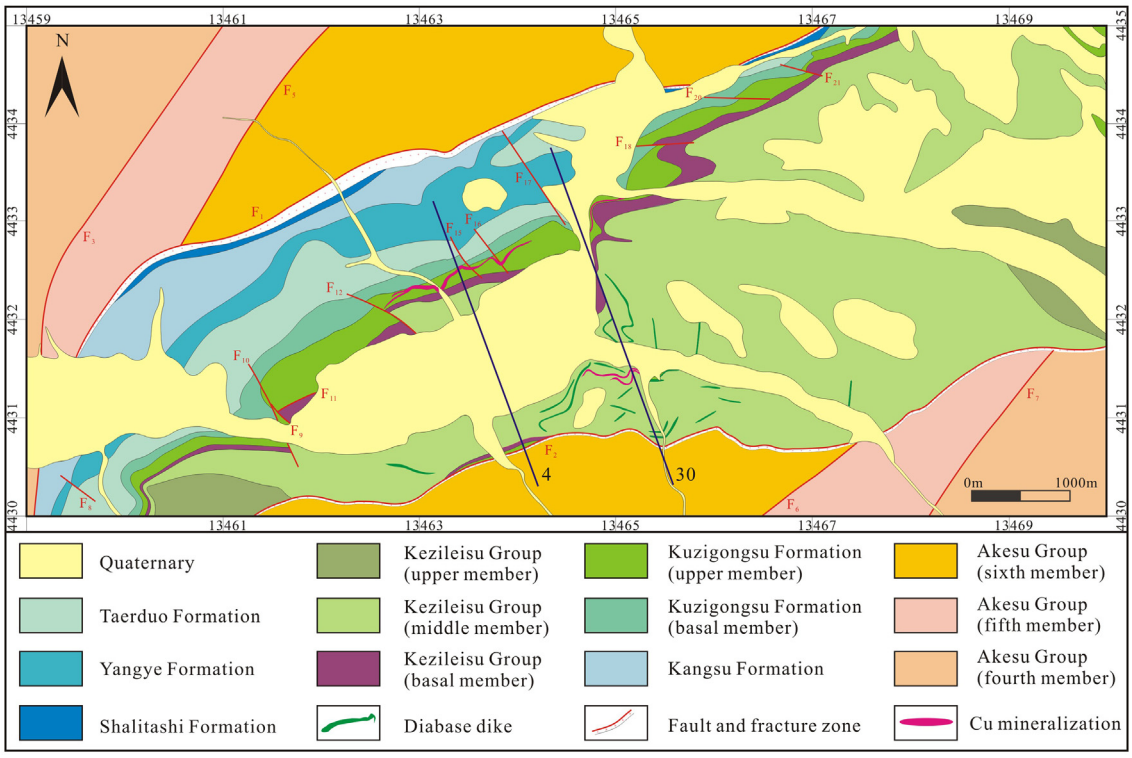

Fig. 2. Geologic map of the Suoerkuduke district (modified after Jia et al., 2016). Geologic cross-sections of Exploration Line 4 and 30 are shown in Fig. 4.

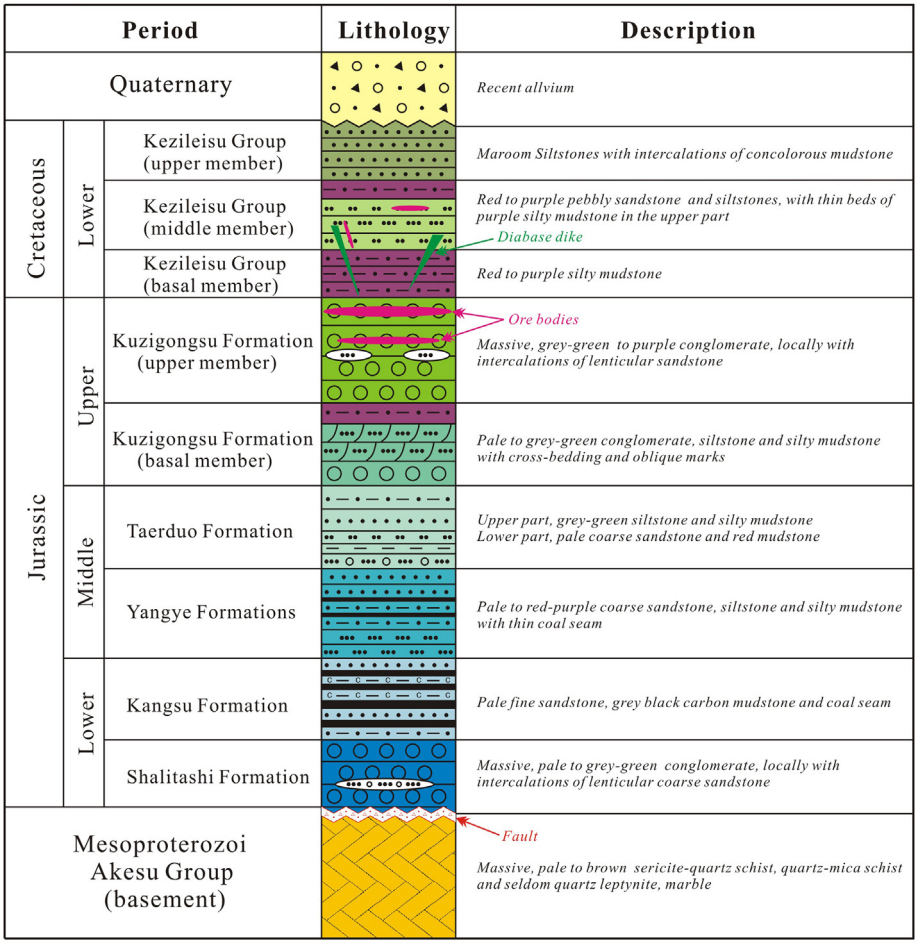

Fig. 3. Stratigraphy and major lithologies of the Sarekbayi basin along with the lithostratigraphic location of major orebodies.

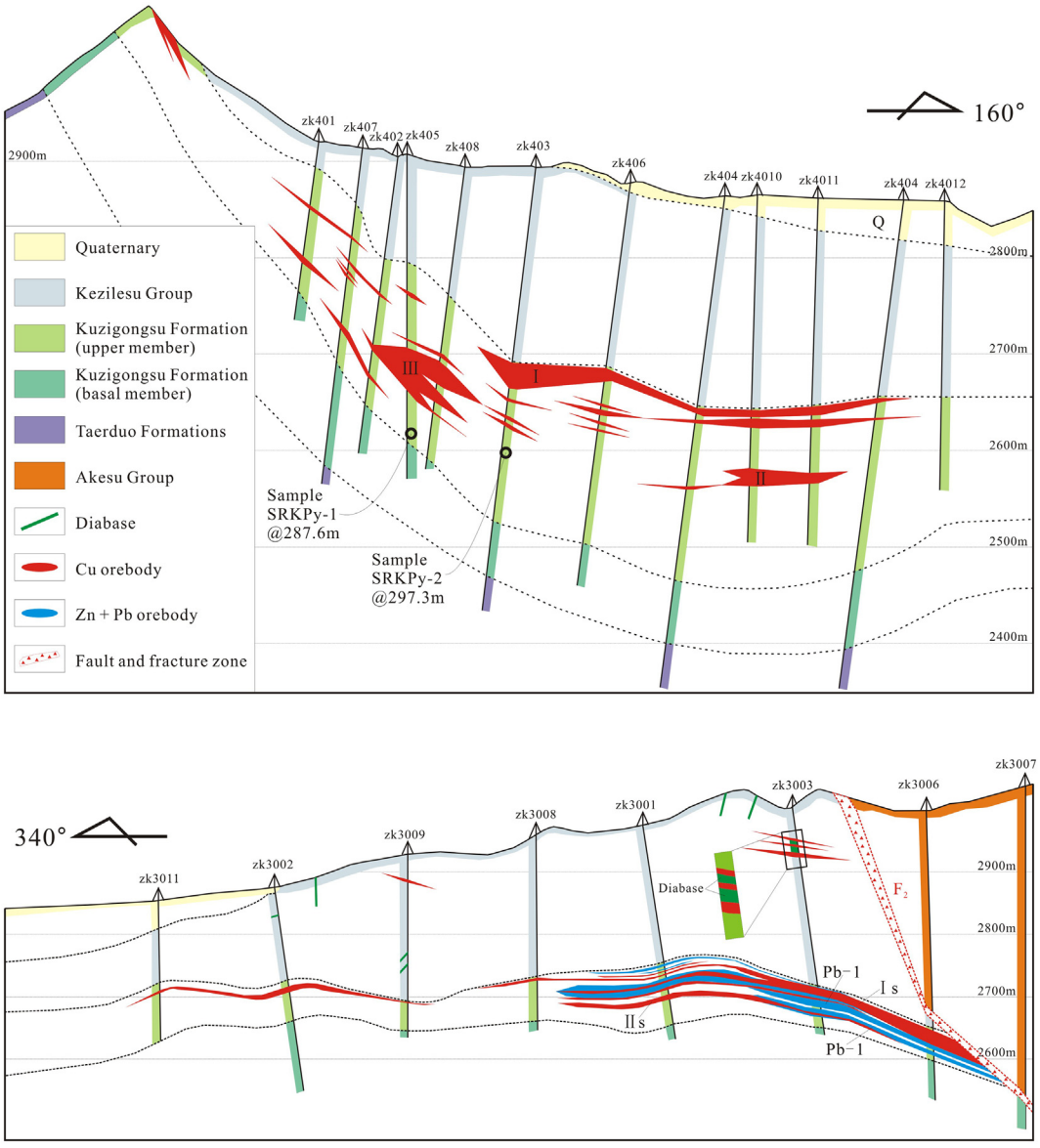

Fig. 4. Cross sections of the Exploration Line 4 (top) and 30 (bottom) (modified after Liu et al., 2016). Location and orientation of the sections are shown in Fig. 2.

middle members of the Kezilesu Group (Fig. 5A) or along the bedding of the middle member of the Kezilesu Group. These dikes are grey-green with typical ophitic texture, and are crosscut by the pyrite/chalcopyrite bearing carbonate ± quartz veins (Fig. 5B), indicating the diabase dikes were pre-mineralization.

3.2. Alteration and mineralization

Mineralization at Sareke is predominantly stratabound and occurs as stacked arrays of lenticular bodies ranging from one to tens of meters thick and of 2.5 km long. The majority of the ores are hosted in conglomerate of the upper member of Kuzigongsu Formation, and minor (sub-economic) in pebbly sandstone of the middle member of the Kezilesu Group. Bound by the Sarekebayi synclinal axis, the southern ore zone contains copper together with minor lead and zinc mineralization, whereas the northern part only contains copper orebodies (Fig. 4).

The carbonatization is the most extensive hydrothermal alteration at Sareke, which occurs as carbonate cement in sandstones and conglomerates, and that replace matrix and calcareous cements as well as framework grains (Fig. 5C). Along with the carbonatization process, the color of wall rocks changed from red-purple into grey-white (sandstone, Fig. 5D–E) and grey-green (conglomerate, Fig. 5F), respectively, and were accompanied by disseminated Cu mineralization (Fig. 5G–H). In general, the alteration halo of sandstone in middle member of the Kezilesu Group were developed along the diabase dikes (Fig. 5I), and are generally 1–3 m wide.

Silicification was mainly developed in the southern ore zone and was then crosscut or replaced by calcite veins (Fig. 6A–B), indicating it was pre-carbonatation. Chloritization only occurred locally and replaced the carbonate minerals (Fig. 6C), representing the last stage of the hydrothermal alteration at Sareke. The primary sulfide minerals in the ores are mainly chalcocite, bornite, chalcopyrite, pyrite together with minor galena and sphalerite. Most of the pyrites are finely disseminated (Fig. 6D) with carbonates and minor occur as coarse aggregates (Fig. 6E). In the ores, the euhedral pyrites were often replaced by bornite (Fig. 6G), sometimes only pyrite residues were retained (Fig. 6H). The chalcopyrite replaced the bornite and were then replaced by chalcocite or sphalerite (Fig. 6I), indicating the paragenetic sequence of metal mineral precipitation: pyrite → bornite → chalcopyrite → chalcocite/sphalerite. There is no significant supergene-enriched mineralization above the primary sulfide orebodies, whereas a

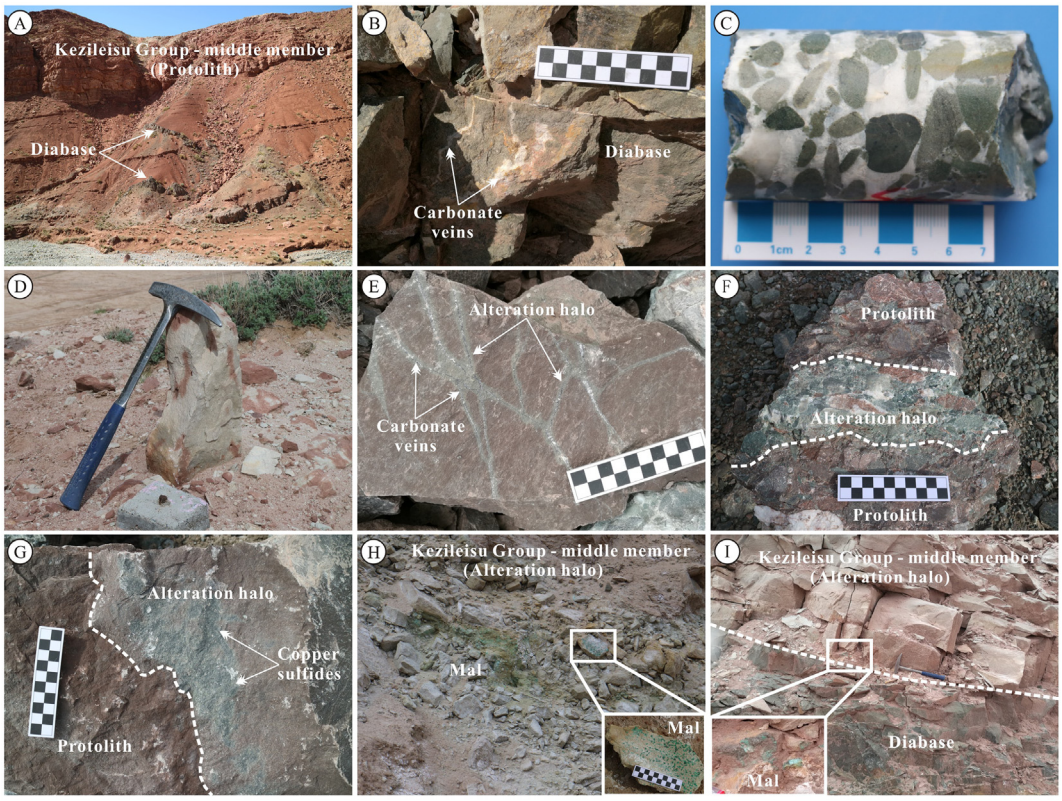

Fig. 5. Diabase and carbonate alteration characteristics of Sareke Cu deposit. (A) The diabase crosscut the middle member of the Kezilesu Group. (B) The diabase was crosscut by the copper sulfide bearing carbonate veins. (C) The pebbles in the conglomerate are cemented by carbonate minerals. (D) The planar alteration of sandstone, the protolith (red) present as porphyritic residual. (E) The veinlet alteration of silty mudstone (basal member of the Kezilesu Group), and the alteration halo is clearly distributed around the carbonate veins. (F) The band alteration of conglomerate and the associated copper mineralization. (G) The planar alteration of conglomerate with disseminated copper sulfides. (H) The fading halo of sandstone (middle member of the Kezilesu Group) was developed along the diabase dike, the inset shows the disseminated copper (malachite) mineralization within the alteration halo. (I) Disseminated copper (malachite) mineralization within the alteration halo of sandstone. Mal – Malachite.

small number of malachite, covellite, chessylite and chalcanthite can still be found in the surface of orebodies.

The Cu ores are dominantly disseminated and minor in carbonate ± quartz veinlets, with metallic minerals including mainly chalcocite (Fig. 6J) and pyrite in the northern zone to chalcopyrite (Fig. 6K), sphalerite, galena (Fig. 6L) and pyrite in southern zone. This gives a mineral zonation pattern of chalcocite → chalcopyrite → sphalerite + galena → pyrite from north to south on the whole. No silver grades or production figures are available at Sareke, but native silver is reported to occur as exsolution within or on the margin of bornite and chalcopyrite (Liu et al., 2016). A summary of paragenetic sequences is shown in Fig. 7.

4. Analytical methods and results

Six pyrite samples were collected for Re-Os dating, of which the samples SRKPy-1 and 2 (Fig. 6D) were collected from drill cores, and their locations were shown in Fig. 4, another four samples (fracture-filling, SRKPy-3 to 6, Fig. 6E) were collected from ore piles. Pyrite in the samples are all cubic euhedral, and coexists with bornite + chalcopyrite ± quartz ± carbonate minerals (Fig. 6F). The samples were crushed and then purely pyrite grains were hand-picked under a binocular microscope. The pyrite grains were crushed in an agate mortar and then were rinsed with Milli-Q deionised water in an ultrasonic bath for at least 20 min.

Re-Os isotope analyses were carried out at the Re-Os Laboratory, National Research Center of Geoanalysis in Beijing, following the method described by Li et al. (2015). Approximately 0.2 to 0.7 g of the pyrite powder was weighed and placed in Carius tubes. The weighted ^{190}Os -^{185}Re spike and 3 ml HCl, 5 ml HNO_3 and 1 ml H_2O_2 were loaded, while the bottom part of the tube was frozen at -50 to -80 °C in an ethanol-liquid nitrogen slush. The top was sealed using a natural gas torch. The tube was then placed in a stainless-steel jacket and heated for 24 h at 230 °C.

After decomposition, the glass tubes were again chilled in a bath of liquid N_2 and ethanol before opening. The osmium was separated by the method of direct distillation from the Carius tube for 50 min, and was then trapped in 5 ml 50% HBr. Then the HBr solution containing Os was purified by the microdistillation method (Creaser et al., 1991). The residual Re-bearing solution was saved in a 150 ml Teflon beaker for Re separation.

The residual Re-bearing solution was heated to near-dryness twice. 10 ml of 25% NaOH was added to the residue followed by Re extraction with 10 ml of acetone in a 120 ml Teflon separation funnel. Discard the water phase afterwards. The acetone phase was washed with 2 ml of 25% NaOH. The acetone phase was transferred to 100 ml beaker with 2 ml H_2O. The liquid was then evaporated to dryness, and picked up in 2% HNO_3. The purified Os and Re were loaded to Pt filaments and analyzed using negative ion thermal ionization mass spectrometry (NTIMS), using a second electron multiplier (SEM) in peak-hopping mode for Os and by static Faraday collectors for Re. Measured Re and Os isotopic ratios were corrected for isobaric oxygen interferences, mass fractionation using $^{185}Re/^{187}Re = 0.59738$, and $^{192}Os/^{188}Os = 3.08271$ (Li et al., 2015).

The Chinese certified reference materials (JCBY sulfide), and one sample blank was used for data quality control. Average blanks for the method are ~1.4 pg Re and ~0.09 pg Os. The sample GBW04477 (JCBY) contains Re content and $^{187}Os/^{188}Os$ ratio of 37.99 ± 0.28 ppb

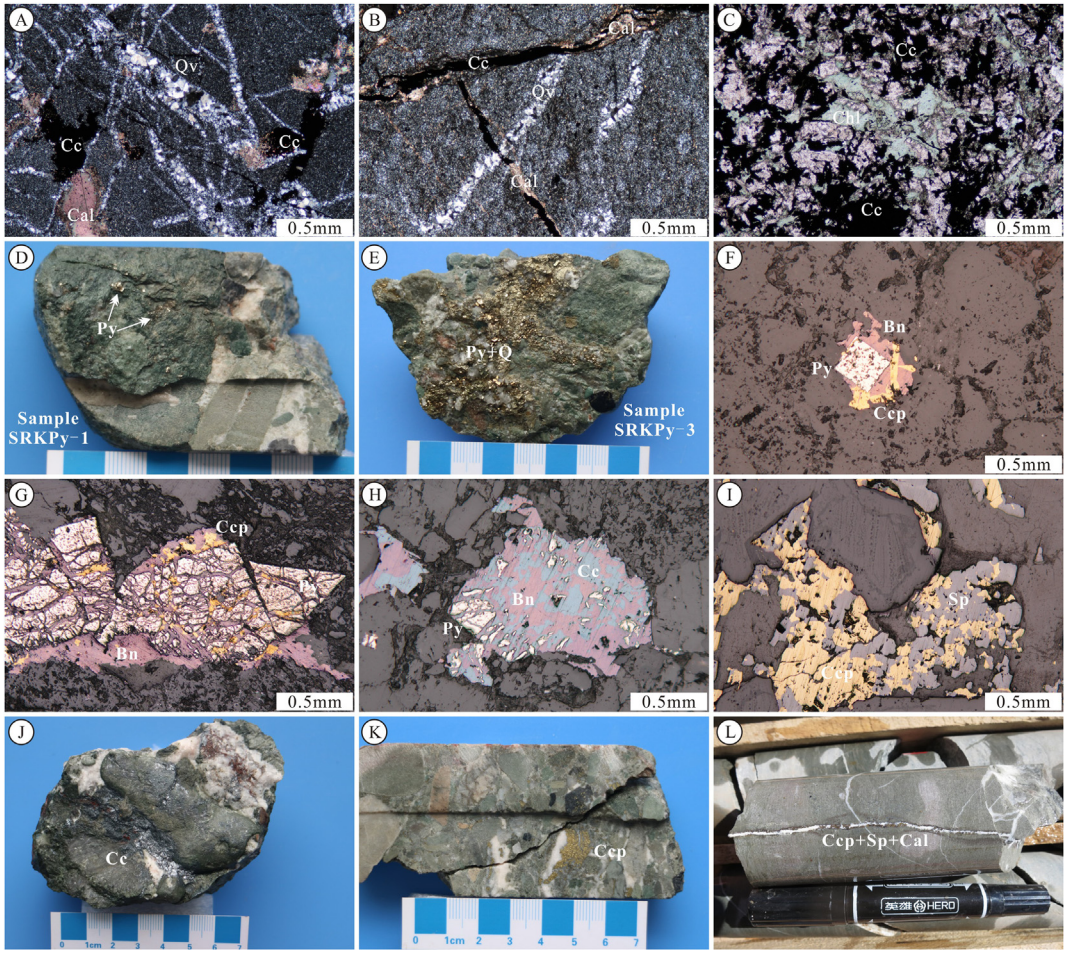

Fig. 6. Mineralization characteristics of the Sareke deposit. (A) Silicification occurs as stockworks and were crosscut by calcite veins. (B) Quartz veins were crosscut by calcite veins. (C) The chlorite replaced the calcite. (D) Typical conglomerate-hosted, disseminated euhedral pyrite. (E) Crystalline pyrite. (F) Euhedral pyrite intergrown with bornite and chalcopyrite. (G) The cubic pyrite was replaced by bornite and chalcopyrite. (H) The bornite was replaced by chaococite, only pyrite local residues were retained. (I) The chalcopyrite was replaced by sphalerite. (J – K) Typical conglomerate-hosted, disseminated chalcocite and chalcopyrite mineralization. (L) Typical carbonate veinlet chalcopyrite + sphalerite mineralization. Qv – Quartz veins; Cal – Calcite; Chl – Chlorite; Py – Pyrite; Bn – Bornite; Ccp – Chalcopyrite; Cc – Chalcocite; Sp – Sphalerite.

and 0.3369 ± 0.0008, respectively, consistent with the certified values of 38.61 ± 0.54 ppb and 0.3363 ± 0.0029 (Du et al., 2013). Uncertainties were determined by those of the blank, the ^{187}Re decay constant of 1.666×10^{-11} a^{-1} (Smoliar et al., 1996), the ages were plotted using Isoplot v 3.0 (Ludwig, 2003).

The Re and Os isotopic compositions of pyrite from the Sareke Cu deposit are shown in Table 1. The Re abundances of pyrite range from 1.919 to 20.299 ppm, with ^{187}Re and ^{187}Os ranging from 1.206 to 12.758 ppm and 2.264 to 24.98 ppb, respectively. The six pyrite grains yielded a well-constrained isochron age of 115.8 ± 4.7 Ma (MSWD = 3.9; Fig. 8A), and a weighted mean age of 114.3 ± 1.8 Ma (MSWD = 2.9; Fig. 8B).

5. Discussion

The formation of Tuyon basin was likely the result of Jurassic to Early Cretaceous reactivation of Talas-Fergana fault (Koserav et al., 1993; Allen et al., 2001; Luo et al., 2004, 2005). Its evolution history had been studied in detail by Liu et al. (2016) and was summarized below:

At the onset of Early Jurassic, along with the rapid rifting, the alluvial fan facies conglomerate may have deposited first followed by the continuing subsidence. A succession of lacustrine-bog facies coal series was deposited in the late Early Jurassic. During the climax of rift stage, semi-deep and deep lacustrine sandstone and mudstone were deposited in the Middle Jurassic. Due to the Late Jurassic rapid subsidence, the alluvial fan facies conglomerate of the red-bed sequence (Kuzigongsu Formation), which host the Sareke Cu mineralization, was deposited. From the Early Cretaceous, the rifting of Talas-Fergana diminished gradually, and accordingly the Tuyon basin changed into a braided river depositional environment, which involve the seal sequence (Kezilesu Group) above the basal red-bed sequence. The late Early Cretaceous is an important transition period, during which the Tuyon basin transformed from extension into uplift, accompanied by extensive basaltic magmatic activities.

The geologic features, especially the carbonate alteration and the veinlet-type mineralization, clearly indicate that the sulfides were precipitated after the sedimentation, and this was further demonstrated by the pyrite Re-Os data, which yielded a well-constrained late Early Cretaceous isochron age of 115.8 ± 4.7 Ma and a weighted mean age of 114.3 ± 1.8 Ma, We interpret the weighted mean age of 114.3 ± 1.8 Ma to represent the Cu mineralization age at Sareke, which was coeval with the timing of Tuyon basin inversion, an important period for SSC mineralization (Hitzman et al., 2005, 2010, 2012).

The diabase dikes contain Cu sulfides- carbonate-quartz veinlets, in common with the surrounding gray-white sandstone and the gray-green conglomerate. Meanwhile, the alteration zones of sandstone that with

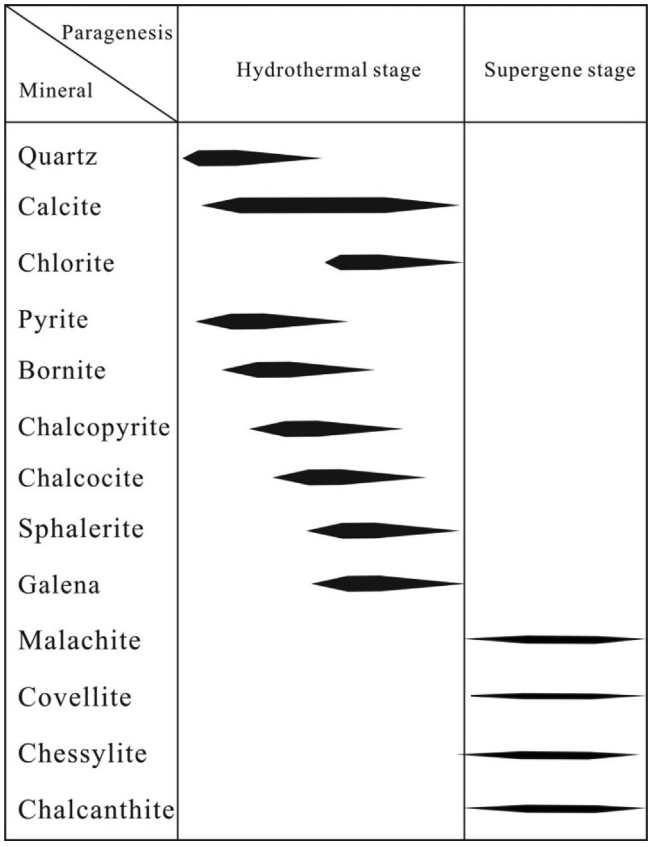

Fig. 7. Paragenetic sequence of minerals at Sareke deposit.

disseminated copper mineralization developed along the diabase dikes. These observations require that the copper mineralization affected the sedimentary rocks and the mafic dikes at the same time and, hence, that the mineralization must postdate intrusion. An attempt to date these intrusions by the U-Pb method was unsuccessful because of the lack of zircons. However, geochronology studies revealed that the timing of mafic magma activities in the Tuyon basin were concentrated on two episodes, the late Early Cretaceous (120 – 104 Ma, Li et al., 1995; Han et al., 1998; Sobel and Arnaud, 2000; Xu et al., 2003) and Paleogene (70 – 48 Ma, Wang et al., 2000; Ji et al., 2006; Liang et al., 2007), with the former peaked at around 112 Ma (Xu et al., 2003). The field evidence confirms that the diabase dikes were intruded during the late Early Cretaceous. The close space-time correlations suggest a genetic link between the Cu mineralization and the diabase intrusion, whereas the Pb-S isotopic compositions indicate that sulfur of ores mainly comes from sulfate biological reduction and the ore-forming metals were all sourced from sedimentary rocks (Li et al., 2011). Hence, we propose that the magma activity may have provided heat to drive fluid migration during mineralization process (Hitzman et al., 2005).

Regionally, Jurassic basins (e.g., Turgay, Leontiev, Tuyon and Kezileitao) are widely distributed along the Talas-Fergana fault

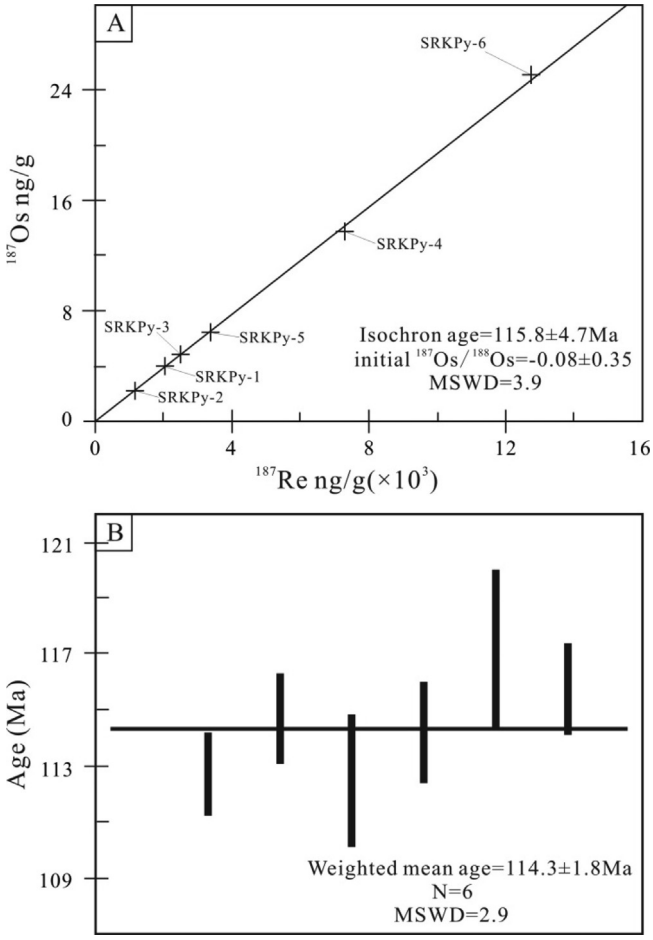

Fig. 8. Re-Os isochron diagrams (A) and weighted average model age diagrams (B) of pyrite samples from Sareke Cu deposit.

(Burtman, 1980; Burtman et al., 1996; Allen et al., 2001; Luo et al., 2005). The geochronology study herein of Early Cretaceous in the Sareke region is the first unequivocal documentation copper mineralization event in these Jurassic basins and will be helpful for the future exploration in the area.

6. Conclusions

The Early Cretaceous pyrite Re-Os age (114.3 ± 1.8 Ma) here provides robust evidence that the Sareke Cu deposit was formed after the deposition of the sedimentary ore host. The contemporary Tuyon basin inversion and mafic magmatism may have been the dynamic and thermodynamic mechanism during the mineralizing process.

Acknowledgements

Special thanks are due to the management and staff of the Sarek

Table 1
Re-Os isotope data for pyrite in the Sareke Cu deposit, Xinjiang.

Sample No.	Weight (g)	Re (μg/g)	Common Os	^{187}Re μg/g	^{187}Os ng/g	Model dates (Ma)
SRKPy-1	0.70000	3.291 ± 0.034	0.0001 ± 0.0008	2.069 ± 0.021	3.998 ± 0.020	115.88 ± 1.78
SRKPy-2	0.20752	1.919 ± 0.016	0.0001 ± 0.0017	1.206 ± 0.010	2.264 ± 0.013	112.59 ± 1.60
SRKPy-3	0.20006	4.014 ± 0.041	0.0001 ± 0.0010	2.523 ± 0.026	4.827 ± 0.028	114.74 ± 1.76
SRKPy-4	0.20482	11.654 ± 0.032	0.0001 ± 0.0017	7.325 ± 0.146	13.72 ± 0.080	112.31 ± 2.57
SRKPy-5	0.20216	5.422 ± 0.071	0.0001 ± 0.0017	3.408 ± 0.045	6.489 ± 0.037	114.19 ± 1.98
SRKPy-6	0.20287	20.299 ± 0.487	0.0001 ± 0.0008	12.758 ± 0.306	24.98 ± 0.150	117.39 ± 3.12

Notes: Uncertainties are given as 2σ absolute variation for Re and Os concentrations.

Nonferrous Group Co. Ltd. for their hospitality and valuable help during field work. The work reported here was funded by the China National Industry Funds (201511016–2), the National 305 Support Program of China (2015BAB05B04–03) and the National Natural Science Foundation of China (41702103, 41602098).

References

Allen, M.B., Alsop, G.I., Zhemchuzhnikov, V.G., 2001. Dome and basin refolding and transpressive inversion along the Karatau fault system, Southern Kazakhstan. J. Geol. Soc. 158 (1), 83–95.

Bazhenov, M.L., Mikolaichuk, A.V., 2000. Paleomagnetism of Paleogene basalts from the Tienshan, Kyrgyzstan: rigid Eurasia and dipole geomagnetic field. Earth Planet. Sci. Lett. 195 (1–2), 155–166.

Burtman, V.S., Skobelev, S.F., Molnar, P., 1996. Late Cenozoic slip on the Talas-Fergana fault, the Tienshan, Central Asia. Geol. Soc. Am. Bull. 108 (8), 1004–1021.

Burtman, V.S., 1980. Faults of Middle Asia. Am. J. Sci. 280 (8), 725–744.

Creaser, R.A., Papanastassiou, D.A., Wasserburg, G.J., 1991. Negative thermal ion mass spectrometry of osmium, rhenium and iridium. Geochim. Cosmochim. Acta 55, 397–401.

Du, N.D., Qu, W.J., Wang, D.H., Li, C., 2013. Re-Os geochronology and its application in ore deposits. Geological Publishing House Publication, Beijing, pp. 233.

Fang, W.X., Jia, R.X., Guo, Y.Q., Li, T.C., Wang, L., Huang, Z.Y., 2016. Hydrocarbon - rich basin fluid with Reductibility and metallogenic mechanism for Glutenite-type Cu-Pb-Zn-U deposits in the Weatern Tarim Basin. J. Earth Environ. 38 (6), 727–752 (in Chinese with English abstract).

Gilder, S., Chen, Y., Cogné, J.P., Tan, X., Courtillot, V., Sun, D., 2003. Paleomagnetic of Upper Jurassic to Lower Cretaceous volcanic and sedimentary rocks from the Western Tarim and implications for inclination shallowing and absolute dating of the M-0 (ISEA?) chron. Earth Planet. Sci. Lett. 206 (3), 587–600.

Han, B.F., Wang, X.C., He, G.Q., Wu, T.R., Li, M.S., Liu, Y.L., Wang, S.G., 1998. Study on the mantle and lower crust xenoliths in the volcanic rocks of Early Cretaceous, Southwestern Tienshan. Chin. Sci. Bull. 43 (23), 2544–2547 (in Chinese).

Hitzman, M.W., Kirkham, R., Broughton, D., Thorson, J., Selley, D., 2005. The Sediment-Hosted Stratabound copper ore system. Econ. Geol. 100th Anniversary Volume, 609–642.

Hitzman, M.W., Selley, D., Bull, S., 2010. Formation of Sediment-Hosted Stratabound Copper deposits through Earth history. Econ. Geol. 105 (8), 627–640.

Hitzman, M.W., Broughton, D., Selley, D., Woodhead, J., Wood, D., Bull, S., 2012. The Central African Copper belt: diverse stratigraphic, structural, and temporal settings in the worlds largest sedimentary copper district. Soc. Econ. Geol. Spec. Publ. 16, 487–514.

Huang, X.W., Zhao, X.F., Qi, L., Zhou, M.F., 2013. Re-Os and S isotopic constraints on the origins of two mineralization events at the Tangdan Sedimentary Rock-Hosted Stratabound Cu deposit, SW China. Chem. Geol. 347, 9–19.

Ji, J.Q., Han, B.F., Zhu, M.F., Chu, Z.Y., Liu, Y.L., 2006. Cretaceous-Paleogene alkaline magmatism in Tuyon basin, Southwest Tianshan mountains: geochronology, petrology and geochemistry. Acta Petrologica Sinica 22 (5), 1324–1340 (in Chinese with English abstract).

Jia, R.X., Fang, W.X., Wang, L., Liu, Z.R., Ye, L., Li, S.Q., 2016. Mineral prediction methods in Sareke copper polymetallic deposit, Xinjiang. Mineral. Explor. 7 (6), 965–970 (in Chinese with English abstract).

Koserav, G.L., Petersen, N.V., Vinnik, L.P., Roecker, S.W., 1993. Receiver functions for the Tienshan analog broadband network: contrasts in the evolution of structure across the Talasso-Fergano Fault. J. Geophys. Res. 98 (B3), 4437–4448.

Li, S.F., Wang, G., 2008. Influences of tectonic events since Mesozoic on Uranium mineralization in Middle-Lower Jur assic of Kashgar Sag. World Nucl. Geosci. 25 (1), 7–12 (in Chinese with English abstract).

Liu, Z.R., Chen, Z.L., Han, F.B., Qi, S.J., Ye, L., Yu, Z.C., Zhu, X.Y., Ren, J.W., Liu, Z.Q., Zhang, L., Yang, Y.X., Hu, Y.P., 2016. Study on optimizing evaluation of prospecting target area for sediment-hosted Cu, Zn and Pb deposits in the West-Tarim District. Beijing Institute of Geology for Mineral Resources, Unpub (in Chinese).

Li, C., Yang, X., Zhao, H., Zhou, L.M., Du, A.D., Li, X.W., Qu, W.J., 2015. High precise isotopic measurements of Pg–Ng Os by negative ion thermal ionization mass spectrometry. Rock Mineral Anal. 34, 392–398 (in Chinese with English abstract).

Li, Y.A., Li, Q., Sun, H., Sun, D.J., Cao, Y.D., Wu, S.Z., 1995. Palaeomagnetic study of Tarim and its adjacent area as well as the formation and evolution of Tarim basin. Xinjiang Geol. 13 (4), 293–376 (in Chinese with English abstract).

Li, Z.D., Xue, C.J., Xin, J., Wang, S.C., Jia, Z.Y., Shi, G.H., Dong, X.F., Shao, X.L., 2011. Geological Characteristics and S, Pb isotope Geochemistry of Sareke Copper Deposit in Wuqia County, Xinjiang. Geoscience 25 (4), 720–729 (in Chinese with English abstract).

Liang, T., Luo, Z.H., Ke, S., Wei, Y., Li, D.D., Huang, J.X., Huang, F., 2007. Shrimp zircon dating of the Tuyon volcanoes group, Xinjiang, and its geodynatic implications. Acta Petrologica Sinica 23 (6), 1381–1391 (in Chinese with English abstract).

Luo, J.H., Zhou, X.Y., Qiu, B., Yang, Z.L., Yin, H., Li, J.L., 2004. Controls of the Talas-Ferghana Fault on Kashi Sag. Northwestern Tarim Basin 25 (6), 584–587 (in Chinese with English abstract).

Luo, J.H., Zhou, X.Y., Qiu, B., Yin, H., Li, J.L., 2005. Mesozoic-Cenozoic five tectonic events and their petroleum geologic significances in West Tarim Basin. Pet. Explor. Dev. 32 (1), 18–22 (in Chinese with English abstract).

Ludwig, K.R., 2003. Isoplot 3.0a—A geochronological toolkit for Microsoft Excel. Berkeley, California, Berkeley Geochronology Center Special. Publication 4, 71 p.

Muchez, P., André-Mayer, A.S., Desouky, H.A.E., Reisberg, L., 2015. Diagenetic origin of the stratabound Cu–Co deposit at Kamoto in the Central African Copper Belt. Miner. Deposita 50 (4), 437–447.

Perelló, J., Clifford, J.A., Creaser, R.A., Valencia, V.A., 2015. An example of synorogenic Sediment-Hosted copper mineralization: geologic and geochronologic evidence from the Paleoproterozoic Nussir deposit, finnmark, Arctic Norway. Econ. Geol. 110 (3), 677–689.

Selley, D., Broughton, D., Scott, R., Hitzman, M., Bull, S., Large, R., Mc-Goldrick, P., Croaker, M., Pollington, N., Barra, F., 2005. A new look at the geology of the Zambian Copper belt. Econ. Geol. 100th Anniversary Volume 965–1000.

Sillitoe, R.H., Perelló, J., García, A., 2010. Sulfide-bearing veinlets throughout the stratabound mineralization of the Central African Copper belt: temporal and genetic implications. Econ. Geol. 105, 1361–1368.

Sillitoe, R.H., 2012. Copper provinces. Soc. Econ. Geol., Spec. Publ. 16, 1–18.

Sillitoe, R.H., Perelló, J., Creaser, R.A., Wilton, J., Dawborn, T., 2015. Two ages of copper mineralization in the Mwombezhi dome, Northwestern Zambia: metallogenic implications for the Central African copper belt. Econ. Geol. 110 (8), 1917–1923.

Smoliar, M.I., Walker, R.J., Morgan, J.W., 1996. Re-Os ages of group IIA, IIIA, IVA, and IVB iron meteorites. Science 271, 1099–1102.

Sobel, E.R., Arnaud, N., 2000. Cretaceous-Paleogene basaltic rocks of the Tuyon basin, NW China and the Kyrgyz Tianshan: the trace of a small plume. Lithos 50 (1–3), 191–215.

Wang, Y.B., Wang, Y., Liu, X., Fu, D.R., Xiao, X.C., Qi, L.S., 2000. Geochemical characteristics and genesis of Late Cretaceous to Paleoene basalts in Tuyon Basin South Tianshan Mountain. Acta Prteologica Et Mineralogica 19 (2), 131–139 (in Chinese with English abstract).

Xu, X.Y., Xia, L.Q., Xia, Z.C., He, S.P., Ma, Z.P., 2003. Geochemistry and genesis of Cretaceous-Paleogene basalts from the Tuyon basin, Southwest Tianshan Mountains. Geochimica 32 (6), 551–560 (in Chinese with English abstract).

Xue, C.J., Chi, G.X., Li, Z.D., Dong, X.F., 2014. Geology, geochemistry and genesis of the Cretaceous and Paleocene sandstone- and conglomerate-hosted Uragen Zn–Pb deposit, Xinjiang, China: a review. Ore Geol. Rev. 63 (2), 328–342.

Zhao, X.F., Zhou, M.F., Li, J.W., Qi, L., 2013. Late Paleoproterozoic sedimentary rock-hosted stratabound copper deposits in South China: their possible link to the supercontinent cycle. Miner. Deposita 48, 129–136.